*Desalination and Water Treatment*
www.deswater.com

doi: 10.1080/19443994.2016.1138890

57 (2016) 24430–24443
November

Taylor & Francis
Taylor & Francis Group

# A comparative study for the removal of aniline from aqueous solutions using modified bentonite and activated carbon

Monireh Tarlani Azar[a], Mostafa Leili[b,*], Fatemeh Taherkhani[a], Amit Bhatnagar[c]

[a]*Department of Environmental Health Engineering, Hamadan University of Medical Sciences, Hamadan, I.R. Iran, emails: monireh.tarlani@yahoo.com (M. Tarlani Azar), fatemeh.taherkhani@yahoo.com (F. Taherkhani)*
[b]*Department of Environmental Health Engineering, School of Public Health and Research Center for Health Sciences, Hamadan University of Medical Sciences, Shahid Fahmideh Ave., Hamadan P.O. Box 65175-4171, I.R. Iran, Tel. +98 81 38380398; Fax: +98 81 38380509; emails: mostafa.leili@gmail.com, m.leili@umsha.ac.ir*
[c]*Department of Environmental Science, University of Eastern Finland, FI 70211 Kuopio, Finland, emails: amit.bhatnagar@uef.fi, dr.amit10@gmail.com*

Received 24 July 2015; Accepted 3 January 2016

---

## ABSTRACT

This study was aimed to explore the potential of modified bentonite as low-cost adsorbent for the adsorption of aniline from aqueous solution. Natural bentonite was modified with hexadecyltrimethylammonium bromide (HDTMA) (referred as HDTMA-Bent herein), a commonly used surfactant, to increase its adsorption potential. The influence of important experimental parameters, including initial aniline concentration, contact time, solution pH, and adsorbent dosage were studied to optimize the experimental conditions. The results showed that with the increase in adsorbent concentration or initial pH value of the solution, the aniline removal efficiency was also increased. The prepared adsorbents were characterized using scanning electron microscopy, Fourier transform infrared spectroscopy, and X-ray diffraction (XRD) analysis. According to XRD analysis, the increase in the microscopic platelets of modified bentonite could be the reason of enhanced adsorption of aniline. The adsorption kinetics followed the pseudo-second-order model and equilibrium data were fitted well with the Langmuir isotherm model. The maximum adsorption capacity of 9.46 mg/g was observed for HDTMA-Bent for aniline removal. To compare the adsorption results with those obtained from commercial activated carbon (AC), similar batch experiments were also conducted. The results exhibited that HDTMA-Bent has a considerable efficiency (more than 83% under the optimum conditions) and its adsorption capacity is about 12.5% as efficient as commercial AC in removing aniline from aqueous solutions. Furthermore, HDTMA-Bent is ca. 40 times cheaper than the AC suggesting that it can be effectively used as a low-cost adsorbent for aniline removal from water.

*Keywords:* Modified bentonite; Activated carbon; Aniline; Adsorption; Surfactant

---

*Corresponding author.

## 1. Introduction

The presence of organic pollutants in industrial wastewaters poses serious threats to the environment and human health which have gained global attention in recent years [1]. Aniline is a simple organic compound with a benzene ring and a $NH_2$ bond. Aniline, as a common primary substance, is extensively used in petrochemicals, dyestuffs, pharmaceuticals, rubbers, pesticides, photographic, agrochemical, paper, and textile industries (as a by-product for the latter one) [2–5].

Aniline has potential mutagenic and carcinogenic effects. It can react easily in the blood to convert hemoglobin into methemoglobin and results in cyanosis [6]. Continued and long-term exposures of aniline can result in anemia, loss of appetite, weight loss, nervous system affects, kidney, liver and bone marrow disorders, and also allergic skin reaction. Keeping in view of toxic effects of aniline, it has been classified as a prior contaminant by most environmental agencies such as United States Environmental Protection Agency (US EPA) and Europe Economic Committee (EEC) [5–7]. Aniline has relatively high solubility in water and can transport in the environment and water source. There are various evidences of its existence in both terrestrial and aquatic environments [1,4,5]. The permissible limits for aniline-containing effluents are very strict in many countries, for example, in China, the discharge standard of aniline in wastewater is 1 mg/L, in Canada, the guideline value of aniline in freshwater is 2.2 μg/L and in New Jersey State, USA, the permissible limit for aniline in groundwater is 6 μg/L [7].

Aniline is chemically stable in the environment and cannot be removed efficiently with the conventional wastewater treatment methods, and therefore, it is necessary to develop robust technologies [6]. Up to now, several processes for the removal of organic compounds from wastewater have been investigated, including adsorption [8], biodegradation [9], advanced oxidation processes (AOPs) [10], and photocatalysis methods [11]. These processes can degrade or remove aniline in wastewater to some extent but do not efficiently remove it. Aniline is also not decomposed completely and may create some intermediate products such as p-methyl phenol and carboxyl acid [12]. Among the methods mentioned above, adsorption process is low-cost, effective, simple to design, easy to operate, and unaffected by toxicity, for the removal of toxic organic compounds [1,7]. Activated carbon is the most ancient, well-known and high efficiency adsorbent for the removal of a wide variety of pollutants, however, its use is becoming restricted due to its high-cost and regeneration problems. During the past few decades, many low-cost adsorbents have been examined as alternatives to activated carbon (AC) [3,13–15].

Natural mineral adsorbents such as bentonite have shown potential for the removal of organic contaminants [16,17]. Bentonite is extensively used as an adsorbent due to its high specific surface areas, low-cost, and abundance in most soils. In recent years, natural bentonite has been modified by various modifying agents in order to improve its potential for the adsorption of organic pollutants via decreasing surface negative charge and producing large amount of exchangeable positive ions [3]. The known modifiers usually are quaternary ammonium salts with long chain or other cationic surfactants [18,19]. These compounds are known to change the hydrophilic silicate surface of clay minerals to a hydrophobic surface and the obtained complex is referred as organoclay. As a result, organoclay complex is an excellent adsorbent for the removal of organic and inorganic contaminants from aqueous solutions [20].

Therefore, the objective of this study was to modify the natural bentonite with a frequently used surfactant, hexadecyltrimethylammonium bromide (HDTMA) (referred as HDTMA-Bent herein) for enhanced aniline removal and to obtain the basic information about kinetic and equilibrium mechanisms of aniline adsorption through batch experiments. The adsorption conditions were optimized by studying the effect of different physicochemical parameters such as initial aniline concentration, contact time, solution pH, and adsorbent dose. The experimental data obtained from the experiments was fitted to two well-known isotherm models, i.e. the Langmuir and Freundlich models to find the better correlation. The optimum conditions for achieving high aniline removal efficiency in batch adsorption system were also determined using the statistical method. The aniline adsorption performance of modified bentonite was also compared with commercial AC and the results are presented herein. The adsorbents were also analyzed by scanning electron microscope (SEM), FTIR, and X-ray diffraction (XRD) to gain an insight into the physicochemical properties of the adsorbents.

## 2. Material and methods

### 2.1. Materials

The bentonite used in this study was provided from bentonite mines of Zanjan province (west of Iran). For the exchange of inorganic ions with organic cations, hexadecyltrimethylammonium bromide [HDTMA;

$CH_3$-$(CH_2)_{15}$-$N^+(CH_3)_3$] was used, which, along with other required chemical compounds such as aniline ($C_6H_5NH_2$; CAS no: 57-09-0), were purchased from Merck Co., Commercial AC, as untreated and granular was supplied by Sigma-Aldrich.

### 2.2. Preparation of modified bentonite

#### 2.2.1. Preparation of Na-Bent

Initially, Ca-bentonite was mechanically ground and passed through 0.15 mm mesh sieve. Twenty grams of Ca-bentonite was added to 1 M $Na_2CO_3$ solution and agitated with a magnetic stirrer for 3 h at 800 rpm at room temperature. In order to dissolve $CaCO_3$, concentrated HCl (ACS reagent grade) was added dropwise as long as most of the calcium carbonate was dissolved. Then, the solid particles were separated from the mixture by filtration, using Whatman no. 42 filter paper, and washed several times with deionized water until the particles became chloride free as indicated by $AgNO_3$ solution. The product was dried at 110˚C for 24 h in an oven and designated as Na-bentonite [20].

#### 2.2.2. Preparation of HDTMA-Bent (organo-bentonite)

Twenty grams of Na-Bent was dispersed into 200 mL of 4% HDTMA solution and agitated for 24 h. The cationic surfactant, i.e. HDTMA could be adsorbed on the negatively charged surfaces of Na-Bent to form HDTMA-Bent with the capabilities that has not been influenced with the solution pH [21]. Then the bentonite was separated from the solution by filtration and washed several times with deionized water. After washing, the pretreated mineral was dried at 70˚C and stored in dark polyethylene containers [20].

### 2.3. Detection of aniline concentration in synthetic samples

Aniline concentration was analyzed by UV–vis spectrometer (DR-5000, Hach) at a wavelength of 286 nm [22]. However, to validate the results, maximum wavelength absorbance and several solutions with known concentrations of aniline were checked by high-performance liquid chromatography (HPLC) with a solvent phase consisting of water–acetonitrile solution.

### 2.4. Batch adsorption experiments and kinetics studies

The adsorption of aniline on bentonite was studied at room temperature (25 ± 2˚C) with shaking speed of 60 rpm in batch mode. In order to assess the effects of main parameters (effect of solution pH, initial aniline concentration, contact time, and adsorbent dose) on the adsorption of aniline, batch experiments were conducted with raw and modified bentonites, and AC as well. For this purpose, 100 mL of aniline solutions of known concentrations were taken in a 200 mL conical flask (with airtight cap) and pH was adjusted to desired value using 0.1 N HCl or NaOH. After that, known (desired) dosages of adsorbents (both bentonite and AC) were added to the aniline solutions and the suspensions were vigorously agitated by a magnetic stirrer at room temperature for different contact times. After pre-determined time intervals, supernatant solutions were sampled and centrifuged at 15,000 rpm for at least 15 min. Lastly, the supernatant was filtered through a 0.45 μm cellulose acetate filter (Sartorius, Germany) and the concentration of aniline was measured to simply calculate residual aniline concentration and corresponding adsorption efficiency using Eq. (1):

$$R(\%) = \left(1 - \frac{C_t}{C_0}\right) \times 100 \tag{1}$$

where $C_0$ and $C_t$ are the initial and final concentrations of aniline, respectively.

The initial aniline concentration was 300 mg/L for all experiments except for the experiments conducted to evaluate the effect of initial aniline concentration. For kinetics studies, 30 g of HDTMA-Bent and 4 g of AC were equilibrated with 100 mL of aniline solutions in a beaker, as carried out in previous step. In all kinetic experiments, pH of the solution was kept at optimum value. To ensure that standard deviation was less than 10%, experiments were conducted in triplicate. The aniline uptake, $q$ (mg aniline/g modified bentonite or AC), was determined using Eq. (2):

$$q = \frac{(C_0 - C_t) \times V}{m} \tag{2}$$

where $C_0$ and $C_t$ are initial and final concentrations of aniline (mg/L), respectively, $V$ is the volume of solution (L), and $m$ is the adsorbents (dry) mass (g).

To assess and compare the performance of kinetic and isotherm models, the predicted vs. experimental values were evaluated by comparing chi-square statistic ($\chi^2$), which can be described by the following equation and is recommended as an appropriate statistic means for comparing the models with two parameters [23]:

$$\chi^2 = \sum \left[ \frac{(q_{e,exp} - q_{e,cal})^2}{q_{e,cal}} \right] \tag{3}$$

where $q_{e,exp}$ and $q_{e,cal}$ (mg/g) are the experimental and model estimated adsorption capacities, respectively. A small value of $\chi^2$ means that value calculated from the model is closer to the experimental value, while a large $\chi^2$ indicates large difference between them.

### 2.5. Determination of the zero point of charge ($pH_{zpc}$)

The $pH_{zpc}$ gives information about the nature of the adsorbent's surface and can be used to determine the quality of the relation between solution pH and aniline adsorption capacity. The zero point of charge of bentonite samples was determined using 0.01 M NaCl as an electrolyte by adding 0.1 N NaOH or 0.1 N HCl solutions. To do the test, 50 mL of the electrolyte was introduced into different beakers and then the solution pH was adjusted to the required value in the range of 2–12. Following the adjustment of pH, 30 g of HDTMA-Bent and 4 g of AC were separately added into each beaker and shaken for 24 h. After 24 h of agitation, adsorbent was filtered and the final pH of the filtrate was measured. By plotting the initial pH vs. the final pH after 24 h, the zero point of charge of adsorbents was determined from the intersection of these curves [24].

## 3. Results and discussion

### 3.1. Characterization of adsorbents

The chemical composition of the bentonite used in the study is presented in Table 1. Oxide of silica is present in the highest amount followed by calcium and alumina in natural bentonite and HDTMA-Bent, respectively. The Na-Bent, HDTMA-Bent, aniline-loaded HDTMA-Bent, as well as AC and aniline-loaded AC were characterized using Fourier transform infrared (Thermo Nicolet AVATAR 360 FTIR, America) in the range of 400–4,000 $cm^{-1}$ (Fig. 1(a) and (b)). As shown in Fig. 1(a), the absorption peaks at 3,600–3,650 $cm^{-1}$ indicate the H–O–H stretching/vibration bands of water molecules weakly hydrogen bonded to the Si–OH, Al–OH–Al surfaces, and to the –OH stretching vibration of adsorbed water, respectively, which are located between the tetrahedral and octahedral layers of the bentonite. After modification of bentonite with HDTMA, the bound water content of the adsorbents were decreased and resulted in the decrease peak areas and intensities [17]. Stretching vibrations of structural hydroxyl group peak appeared at 3,451 $cm^{-1}$. The bands at 2,930 and 2,857 $cm^{-1}$ were attributed to $CH_2$ asymmetric and symmetric stretching mode, respectively. These bands showed that the HDTMA molecules were inserted into the interlayer space of the bentonite [25] and their bending vibrations at 1,478 and 1,385 $cm^{-1}$ were only observed in HDTMA-Bent. The small band at 1,653 $cm^{-1}$ corresponded to the δSiO–H deformation vibration. The intensive band at around 1,057 $cm^{-1}$ can be assigned to in-plane stretching of the Si–O bond. This band is the characteristic of Si–O stretching vibration of cristobalite. The bond around 952 $cm^{-1}$ might be the evidence for the presence of Al–Al–OH deformation [26]. A sharp band at 797 $cm^{-1}$ indicates quartz admixture, silica, and the rocking band in the sample [27]. The Si–O–Al (octahedral layer) and Si–O–Si bending vibrations appeared at 531 and 465 $cm^{-1}$, respectively [25]. Therefore, the frequency vibration mainly at ~3,451, ~2,930, ~2,857, and ~1,478 $cm^{-1}$ results in the development of more active sites which increases the efficiency of modified bentonites for the aniline removal. Weaker peaks of the functional groups of the aniline-loaded HDTMA-Bent rather than those of the cationic surfactant peaks indicate substitution of the aniline molecules by some cationic surfactant species mainly via ion exchange, electrostatic interactions as well as van der Waals forces [28].

Table 1
Chemical composition of natural and HDTMA-bentonite

| Constituents (%) | Natural bentonite | HDTMA-Bent |
|---|---|---|
| $SiO_2$ | 81.93 | 83.93 |
| $Al_2O_3$ | 4.34 | 6.04 |
| CaO | 7.49 | 5.25 |
| $Fe_2O_3$ | 2.15 | 1.50 |
| $SO_3$ | 1.39 | 0.85 |
| MgO | 0.68 | 0.65 |
| $P_2O_5$ | 0.48 | 0.51 |
| Br | – | 0.43 |
| Cl | – | 0.36 |
| $TiO_2$ | 0.26 | 0.19 |
| MnO | 0.1 | 0.06 |
| $K_2O$ | 0.56 | 0.27 |
| Loss on ignition | 6.50 | 16.25 |

As shown in Fig. 1(b), peaks were observed between 3,933 and 3,622 $cm^{-1}$ which can be attributed to the amino and OH groups of phenyl, and water adsorbed on AC. The peaks around 2,377 and 2,357 $cm^{-1}$ correspond to the C–H stretching of methyl groups and C=C stretching vibration of alkyne groups. The band at 1,607 $cm^{-1}$ represents the combination of

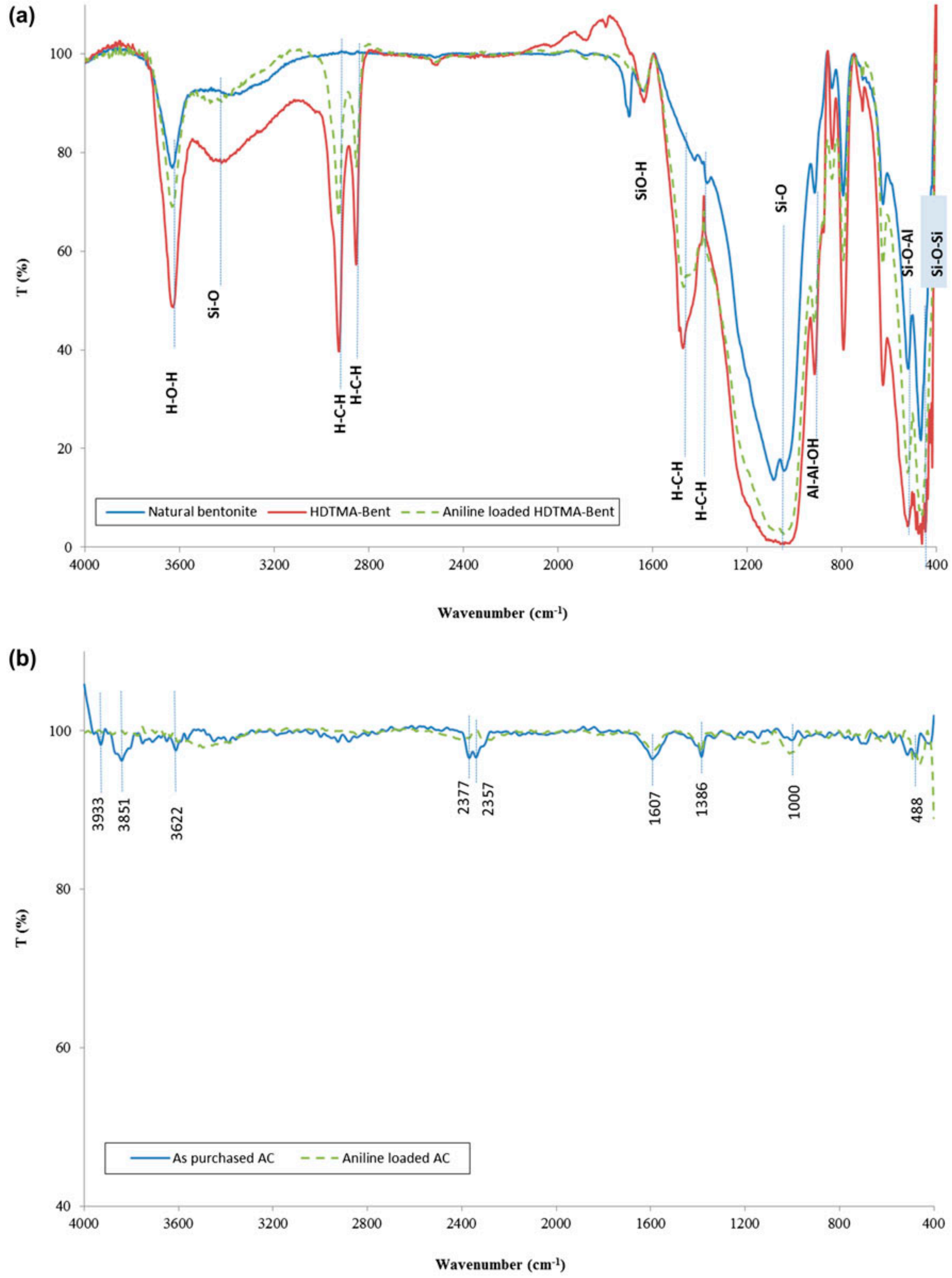

Fig. 1. FTIR spectra of: (a) bentonite and (b) AC.

C=C stretching vibration of the aromatic ring structures. The small band at 1,000 cm$^{-1}$ corresponded to the C–H deformation vibration. The other peaks between 1,400 and 900 cm$^{-1}$ could be attributed to the C–O stretching vibration [29]. The peaks at the region 2,357–3,933 cm$^{-1}$ (characteristic of C=C aromatic skeletal vibrations) appeared to be diminished, indicating the interaction of aniline molecule with the surface of the AC materials [30]. In the adsorbed state, the band appears at 1,000 cm$^{-1}$ may correspond to the strong band of bulk aniline [31].

The $d_{001}$ spacing of adsorbents was measured by XRD to elucidate the structural and mineralogical aspects of intercalated clay minerals in bentonite samples (Fig. 2). The $d_{001}$ spacing of Na-bentonite, which illustrates the amorphous nature of the adsorbents, is 11.41 Å corresponding to the 6.3° (2$\theta$) value attributing to the montmorillonite. The other peaks correspond to quartz and feldspar. The position of the $d_{001}$ peak of HDTMA-Bent shifts to 16 Å and 5.9° (2$\theta$) accompanied by an intensity decreased from 55 to 29%. The increase of basal spacing from 11.41 to 16 Å was caused due to the intercalation of HDTMA molecule onto the interlayer space of bentonite which expanded its interlamellar spacing which in turn promotes aniline removal. The elemental analyses of natural and modified bentonites were also conducted to probe the presence of surfactant in the bentonite interlayer and the results are provided in Table 1. Koyuncu et al. [32] also showed that interlayer spacing of the original bentonite increased from 14.97 to 21.96 Å through the nonionic and cationic surfactants modification of bentonite. The position of the $d_{001}$ peak of aniline-loaded HDTMA-Bent shifts to 6.36 Å. The XRD patterns revealed that the crystal structure of the adsorbent significantly changed after the adsorption of aniline and the increase in the microscopic platelets of modified bentonites could be the reason for higher adsorption of aniline [27].

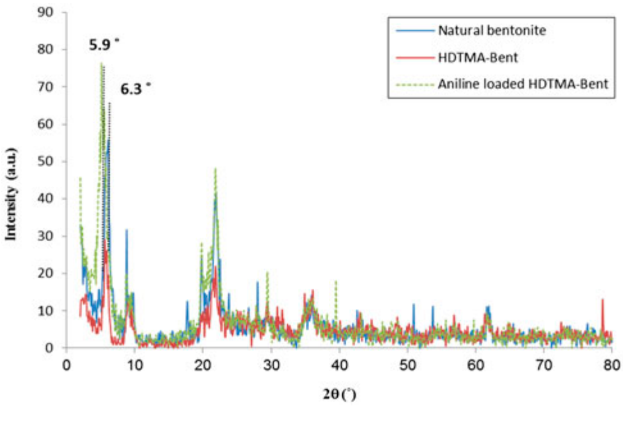

Fig. 2. The XRD pattern of adsorbents.

A SEM equipped with an energy dispersive X-ray microanalysis (LEO-1430 VP) with the accelerating voltage set to 26 kV was used to determine the surface morphology and the porous structure of the adsorbents and the results are shown in Fig. 3. As can be clearly seen, mesoporous structures exist in both adsorbents but these structures were not observed in the raw bentonite (figures not shown here). Furthermore, HDTMA-Bent (Fig. 3(a)) has an irregular morphology and there are many spherical aggregates indicating a smooth surface with scattered cavities and bumps. In fact, the surfactant activation resulted in leaching of cations, making the clay surface more porous which in turn, various sizes of bumps on the surface of the adsorbents make it a well-supported material due to the fact that the presence of this structures on the surface increases the chance of aniline molecules to be trapped and adsorbed onto the surface of the adsorbents. As shown in Fig. 3(c), AC seems to have similar surface properties with many cavities and channels and the effect of porosity on its surface is clear which in turn, provided many tunnels that can help the diffusion of aniline into them. Fig. 3(b) and (d) show the SEM image of aniline-loaded adsorbents. It can be clearly seen that these cavities were filled with adsorbed aniline. The difference in surface morphology of HDTMA-Bent and AC can be attributed to specific base materials as well as to their strength and texture composition.

## 3.2. Effect of operating variables on the adsorption of aniline

### 3.2.1. Effect of initial aniline concentration

The effect of initial aniline concentration on the adsorption process was investigated in the range of 50–1,000 mg/L (shaking speed = 60 rpm, and temperature ~25°C). As presented in Figs. 4(a) and (b), the uptake of aniline is affected by the initial aniline concentration. As the initial concentration increased, the aniline uptake from aqueous solution was also increased because the initial concentration provides an important driving force to overcome all mass transfer resistances of aniline between the aqueous and solid phases. At lower concentrations, the number of available adsorption sites are relatively high, therefore, the aniline molecules were easily adsorbed but at higher initial concentrations, these sites were limited which resulted in the decrease of aniline removal efficiencies [7].

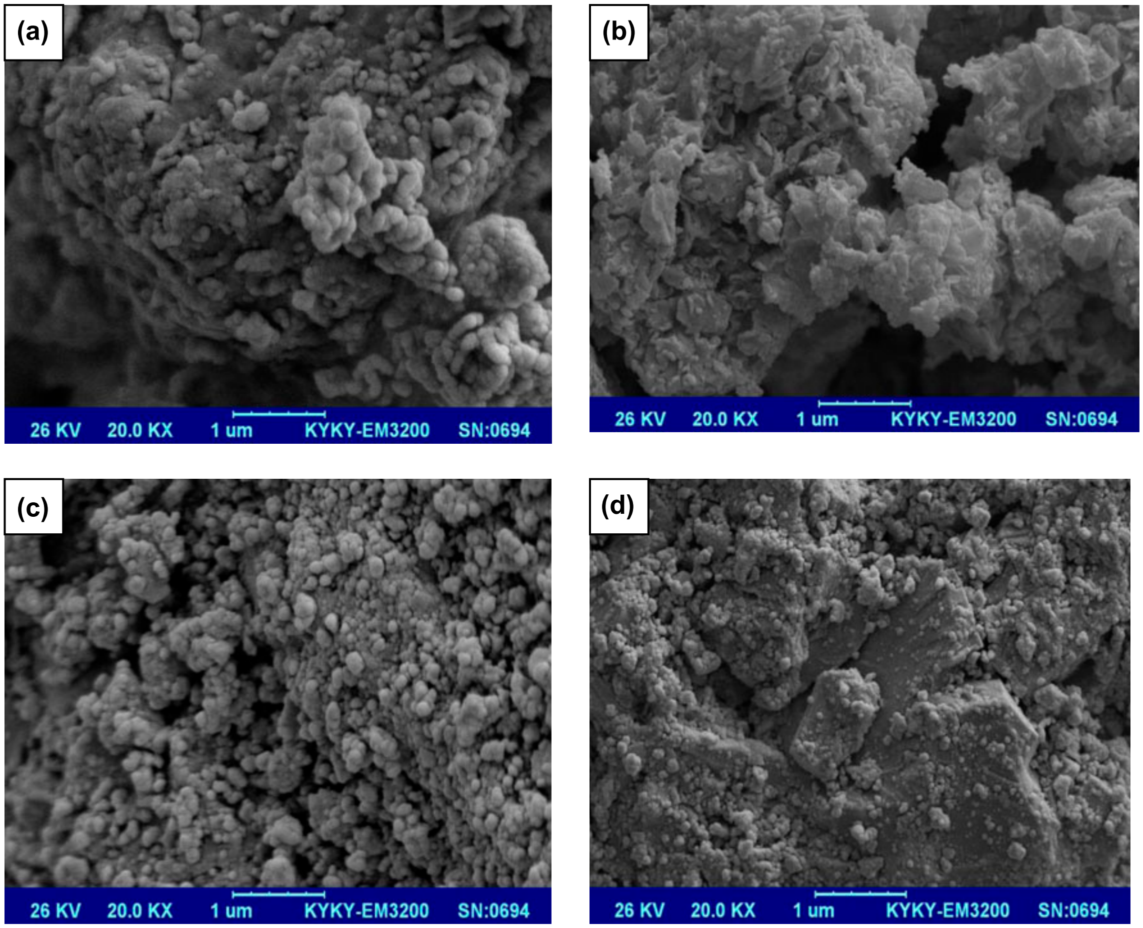

Fig. 3. SEM micrograph of (a) HDTMA-Bent, (b) aniline-loaded HDTMA-Bent, (c) as purchased AC, and (d) aniline-loaded AC.

### *3.2.2. Effect of solution pH*

The solution pH is an important parameter which influences most of the solid/liquid adsorption processes. The adsorption of aniline on the adsorbents was examined at different pH and results are presented in Fig. 5. It was observed that for both adsorbents used in the study, aniline adsorption was increased with the increase in solution pH. For example, as it can be seen from Fig. 5, the adsorption of aniline was increased in case of HDTMA-Bent and the uptake capacities ($q_e$) were observed as 2.83, 7.42, 8.12, and 8.39 mg/g at pHs 2, 8, 10, and 12, respectively. This trend was also observed for AC except that maximum adsorption was observed at pH 10 with value of 63.94 mg/g with the little difference at pH 8 (63.84 mg/g). Since ionizable phenolic compounds (IPC) can exist as different species, ionic or electrically neutral, therefore, solution pH is an important factor that affects interaction of aniline with the adsorbent surface. Aniline is an IPC with weak base nature that could be protonated and form positive ions at pH values lower than its p$K_a$ (5.2) [2]; whereas at pH higher than its p$K_a$ value, aniline molecules are present in neutral or even in some negatively form. Furthermore, bentonites were modified by cationic surfactant and mainly have positive surface charges which are not influenced by solution pH [25,33]. Therefore, the neutral or negatively charged aniline could be better adsorbed onto adsorbents of positively charged surfaces [2]. The effects of solution pH on the removal of aniline can also be explained by considering both factors, viz.: (i) the surface charge of the adsorbents which is related to $pH_{zpc}$ of the adsorbents and (ii) the dissociation constant (p$K_a$) of aniline. The variation in the solution's pH can lead to change in both the surface charge and the functional groups chemistry of the adsorbents' surface. Since the $pH_{pzc}$ of HDTMA-Bent and AC were 9.6 and 5.7, respectively (results not

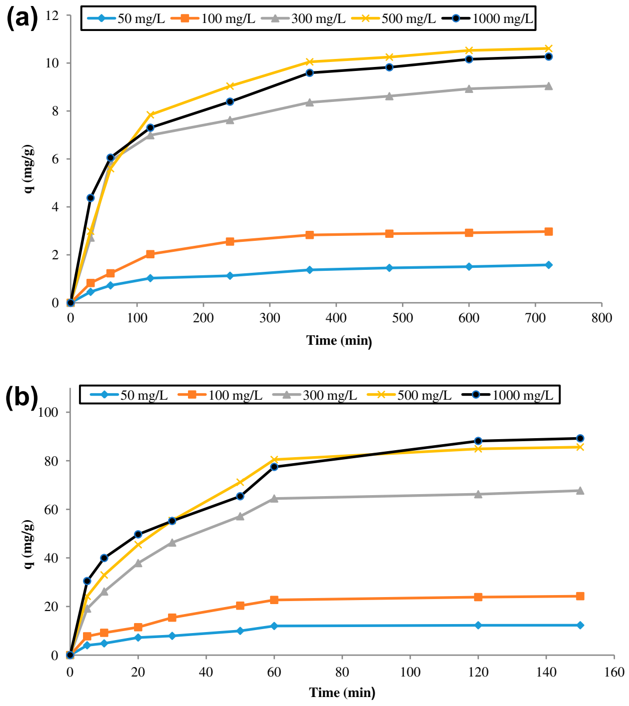

Fig. 4. The effect of initial aniline concentration on the sorption kinetics of (a) HDTMA-Bent (pH 10, adsorbent dose = 30 g/L) and (b) AC (pH 8, adsorbent dose = 4 g/L).

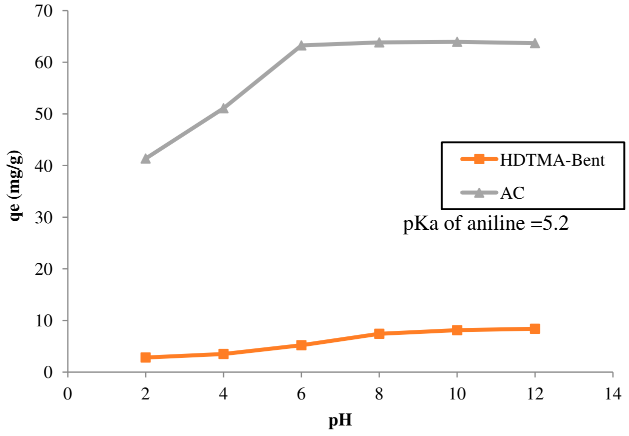

Fig. 5. The effect of solution pH on the removal of aniline from aqueous solution by HDTMA-Bent ($C_0 = 300$ mg/L, adsorbent dose = 30 g/L, contact time = 360 min) and AC ($C_0 = 300$ mg/L, adsorbent dose = 4 g/L, contact time = 60 min).

shown here), a positive charge developed on their surfaces at pH below $pH_{pzc}$, while at higher pH than the $pH_{pzc}$, it becomes negatively charged due to complete deprotonation. Accordingly, the adsorbents used in the study have a relatively high removal efficiency of aniline at pH values <12 and <6 for HDTMA-Bent and AC, respectively. Salam et al. have reported enhanced percent aniline removal by magnetic multi-walled carbon nanotubes/ferrite nanocomposite at pH values of 6–10 [2]. Similar results were reported by Suresh et al. in the study of 4-nitrophenol removal with AC [4] and by Al-Asheh et al. for the phenol adsorption with different types of modified bentonites [34]. As there were only minor differences in the removal efficiencies at pH values 10 and 12 and take in to accounts the operational consideration, therefore, pH 10 was selected as an optimum pH. For the similar reasons, pH 8 was selected as an optimum pH for AC for further study.

### *3.2.3. Effect of contact time*

In order to determine the equilibration time for maximum adsorption of adsorbate and to study the kinetics of adsorption process, the adsorption of aniline on bentonite and AC were studied as a function of contact time and the results are shown in Figs. 6(a)–(c). The aniline adsorption onto bentonite increased with time and the equilibrium was achieved in ca. 360 and 60 min in case of bentonite and AC, respectively. However, to ensure equilibrium, the

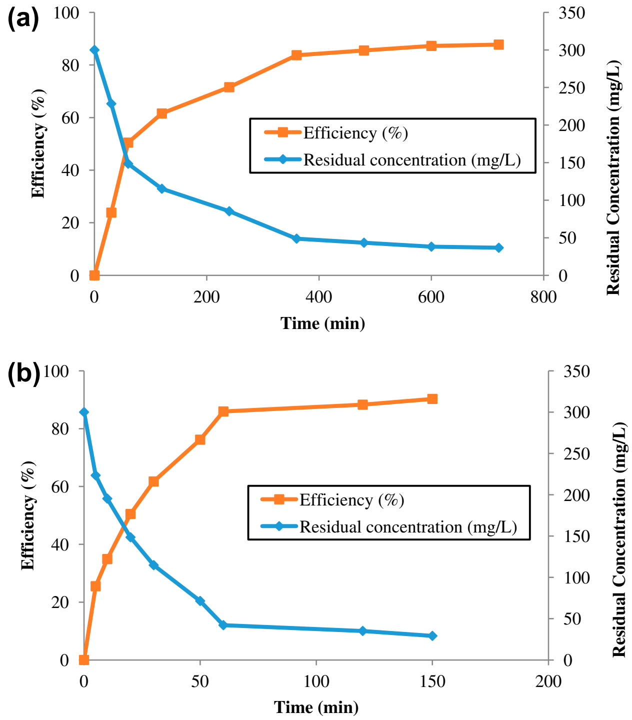

Fig. 6. Effect of contact time for the adsorption of aniline onto (a) HDTMA-Bent ($C_0 = 300$ mg/L, pH 10, adsorbent dose = 30 g/L) and (b) AC ($C_0 = 300$ mg/L, pH 8, adsorbent dose = 4 g/L).

samples were shaken for 6 and 48 h for AC and modified bentonite, respectively (results are not shown here). It was found that during the initial stage of reaction, many vacant surface sites were available for the adsorption and the adsorption rate was also rapid so most of the solutes were adsorbed within the first 360 and 60 min for modified bentonite and AC, respectively; but with the laps of time, an equilibrium was achieved as most of the available sites were occupied by the adsorbate (aniline). [35]. Koyuncu et al. have reported that the equilibrium time of nitrophenols adsorption onto HDTMA- and PEG-modified bentonites was 2 and 8 h, respectively [32]. In the study conducted by Xin et al. [25], the equilibrium time for adsorption of benzoic acid from aqueous solution by various modified bentonites was 90 min. Equilibrium time of 6 h was determined by Anirudhan and Ramachandran [36] for the removal of 2,4,6-trichlorophenol from water and petroleum refinery industry effluents using surfactant-modified bentonite.

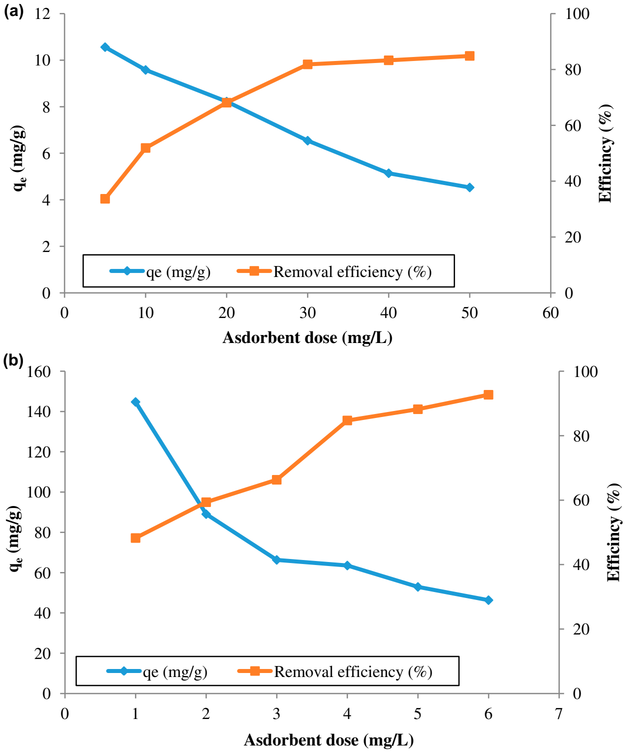

Fig. 7. Effect of adsorbent dose on the adsorption of aniline onto (a) HDTMA-Bent (pH 10, contact time = 360 min) and (b) AC (pH 8, contact time = 60 min).

### 3.2.4. Effect of adsorbent dose

The adsorption of aniline on both HDTMA-Bent and AC was studied by varying the dose of adsorbents from 10 to 50 g/L for HDTMA-Bent and 1 to 6 g/L for AC while keeping other parameters in the optimum ranges. As shown in Fig. 7(a), by increasing the dose of HDTMA-Bent from 10 to 30 g/L, the removal of aniline also increased, but after 30 g/L, the removal was negligible, so, this value was selected as optimum dose to continue the experiments. This may be due to the fact that the increase in adsorbent amount resulted in more available adsorption sites for the adsorbate [25,33,37]. Furthermore, regarding that adsorption mechanism is a function of the solubility and polarity of the organic compounds in aqueous solutions and that the surface of HDTMA-Bent is more hydrophobic, so it enhances the adsorption of compounds that are less soluble in aqueous solution. Accordingly, adsorption increased with the increase in the HDTMA-Bent dose. But beyond the optimum value, the removal efficiency remains constant because, although the reaction sites were increased but the surface and the aniline concentration come to saturation limit with each other and the driving force was not enough to overcome the resistances to the mass transfer of adsorbate between the aqueous and the solid phases [38]. As it is shown in Fig. 7, the $q_e$ also decreased with increasing adsorbent dose. It could be explained by the fact that the adsorbent cannot show its actual potential and capacity in such case as a result of greater number of available sites leading to less competition for adsorption sites [39]. Therefore, the dosage of 30 g/L was used for the further studies of HDTMA-Bent. Similar trend was also observed for AC (Fig. 7(b)).

### 3.3. Adsorption kinetics

Adsorption kinetics can explain the solution uptake rate and reveal the adsorption efficiency of the adsorbents [40]. Kinetics experiments were conducted for HDTMA-Bent and AC in Erlenmeyer's containing 100 mL of aniline solution with three different initial concentrations, pH 10 and 30 g of adsorbent for HDTMA-Bent and pH 8 and 4 g of adsorbent for AC that were agitated at 25°C. After regular time intervals, 5 mL of solution was sampled from the mixtures and aniline's concentration was analyzed until the reaction reached to equilibrium. Two of the most widely used kinetic models namely pseudo-first-order and pseudo-second-order model were applied to understand the adsorption kinetic behavior of aniline onto modified bentonite.

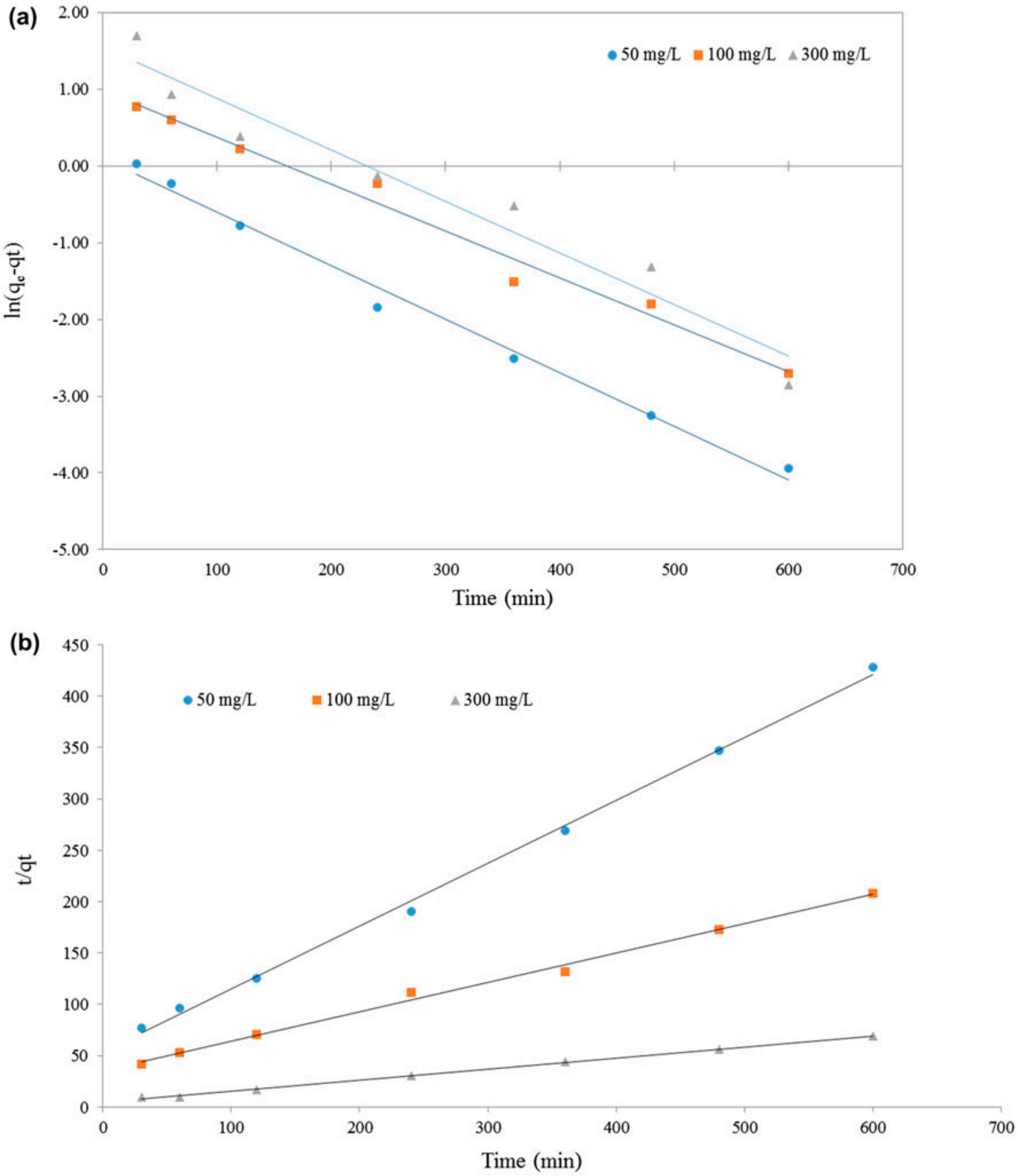

Fig. 8. Linearization of aniline adsorption kinetics on to HDTMA-Bent: (a) the pseudo-first-order model and (b) the pseudo-second-order model (pH 10; adsorbent dose = 30 g/L).

The pseudo-first-order kinetic model is given as Eq. (4) [41]:

$$\ln(q_e - q_t) = \ln q_e - k_1 t \tag{4}$$

where $q_e$ and $q_t$ (mg/g) are the amounts of aniline adsorbed at equilibrium and at time $t$ (min), respectively. The constant $k_1$ (min$^{-1}$) is the adsorption rate constant of pseudo-first-order model, which was determined from the plot of $\ln(q_e - q_t)$ against $t$.

The pseudo-second-order kinetic model is given as Eq. (5) [42]:

$$\frac{t}{q_t} = \frac{1}{k_2 q_e^2} + \frac{t}{q_e} \tag{5}$$

Table 2
Parameters of adsorption kinetic models for the aniline adsorption onto adsorbents

| | Pseudo-first-order | | | | | Pseudo-second-order | | | |
|---|---|---|---|---|---|---|---|---|---|
| Adsorbent | $C_0$ (mg/L) | $k_1$ (min$^{-1}$) | $q_e$ (mg/g) | $R^2$ | $\chi^2$ | $k_2$ (g/mg min) | $q_e$ (mg/g) | $R^2$ | $\chi^2$ |
| HDTMA-Bent | 50 | 0.0069 | 1.24 | 0.991 | 15.71 | 0.0071 | 1.63 | 0.998 | 9.45 |
| | 100 | 0.0062 | 9.67 | 0.984 | 158.22 | 0.0022 | 3.50 | 0.988 | 114.65 |
| | 300 | 0.0071 | 36.31 | 0.949 | 743.59 | 0.0027 | 9.25 | 0.998 | 518.78 |
| AC | 50 | 0.0276 | 131.82 | 0.898 | 35.84 | 0.0043 | 13.83 | 0.993 | 28.32 |
| | 100 | 0.0297 | 905.73 | 0.975 | 211.56 | 0.0018 | 27.70 | 0.991 | 194.43 |
| | 300 | 0.0333 | 1875.47 | 0.958 | 1044.34 | 0.00077 | 72.45 | 0.997 | 998.92 |

where $q_e$ and $q_t$ are defined above, and the constant $k_2$ (g/mg min) is the adsorption rate constant of pseudo-second-order model.

Fig. 8 shows the adsorption kinetics of aniline on HDTMA-Bent, and the results of fitting adsorption data with pseudo-first-order and pseudo-second-order kinetics models and respective parameters are listed in Table 2. As can be seen from the results, the correlation coefficients of pseudo-second-order model were >0.99 for all optimum conditions, and are better (higher) than pseudo-first-order model, indicating that the pseudo-second-order model fitted reasonably well as compared to pseudo-first-order. Therefore, adsorption kinetics of aniline by HDTMA-Bent followed pseudo-second-order model [43]. Table 2 also lists the $\chi^2$ values obtained for the two kinetic models studied. As stated previously, the lower values of $\chi^2$ indicates the better fitting of the results to the tested models. Accordingly, it was found that the pseudo-second-order kinetic model yielded the lowest $\chi^2$ values than those calculated for the pseudo-first-order model. This is also in agreement with the $R^2$ values and proves that the adsorption of aniline onto HDTMA-Bent and AC can be best described by the pseudo-second-order kinetic model.

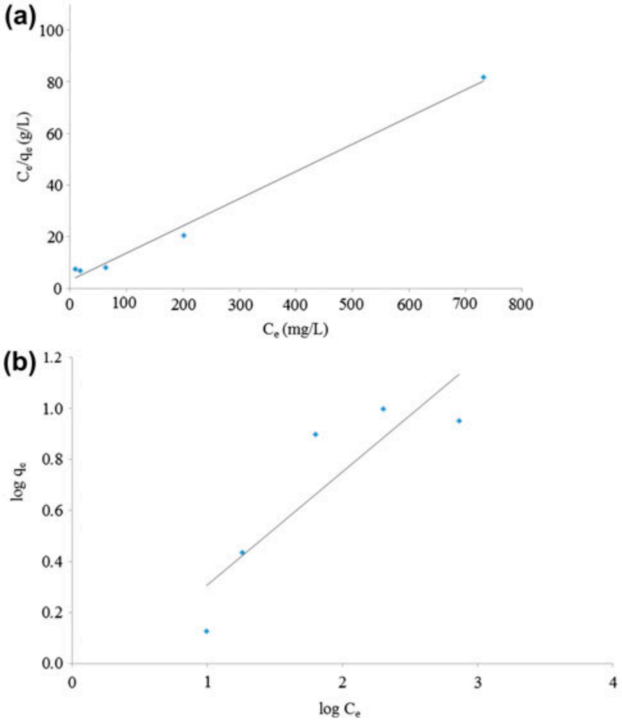

Fig. 9. Adsorption isotherms of aniline on HDTMA-Bent (a): Langmuir model, (b): Freundlich model (pH 10, adsorbent dose = 30 g/L, concentration range: 50–1,000 mg/L).

### 3.4. *Adsorption isotherms*

In order to determine the adsorption mechanisms of aniline on to HDTMA-Bent and AC, Langmuir and Freundlich isotherms models were applied to the experimental data. Langmuir and Freundlich isotherms are the common isotherms used in the equilibrium studies. The isotherm experiments were performed using a series of initial concentrations of aniline (30 and 4 g/L for HDTMA-Bent and AC, respectively).

The Langmuir isotherm assumes that the adsorption takes place in monolayer on a solid surface with a limited number of sites with identical energy and a maximum adsorption correspond to a saturated monolayer of solute molecules on the adsorbent surface. The linearized form of Langmuir is expressed by Eq. (6) [44]:

$$\frac{C_e}{q_e} = \frac{C_e}{q_{\max}} + \frac{1}{q_{\max} K_L} \tag{6}$$

where $C_e$ is the equilibrium concentration of aniline (mg/L), $q_{\max}$ is the maximum aniline adsorbed (mg/g), $q_e$ is the amount of aniline adsorbed per unit weight of adsorbents at equilibrium time (mg/g), and

Table 3
Parameters of Langmuir and Freundlich models for aniline adsorption onto HDTMA-Bent and AC

| | Langmuir isotherm | | | | | Freundlich isotherm | | | |
|---|---|---|---|---|---|---|---|---|---|
| Adsorbents | $q_m$ (mg/g) | $K_L$ (L/mg) | $R_L$ | $R^2$ | $\chi^2$ | $n$ | $K_f$ | $R^2$ | $\chi^2$ |
| HDTMA-Bent | 9.46 | 0.034 | 0.032–0.372 | 0.9916 | 14.23 | 7.42 | 2.77 | 0.7738 | 85.17 |
| AC | 75.76 | 0.115 | 0.008–0.148 | 0.9985 | 1243.67 | 2.94 | 11.48 | 0.8547 | 1786.43 |

Table 4
Comparison of different pollutants removal by bentonite and aniline removal by various adsorbents

| Pollutant | Adsorbent | $q_{max}$ (mg/g) | Refs. |
|---|---|---|---|
| Diazo dye | Bent (Acid activation) | 69.44 | [13] |
| Phosphate | Bent (HO-CaBen) | 29.1 | [17] |
| Nitrate | Bent (Surfactant) | 13.79 | [47] |
| Phenol | Bent (Not modified) | 1.71 | [16] |
| Phenol | Bent (Surfactant) | 8.35 | [34] |
| Arsenic(V) | Bent (Surfactant) | 1.48 | [48] |
| Aniline | Bent (Surfactant) | 9.46 | This study |
| Aniline | Granular activated carbon | 174.93 | [43] |
| Aniline | Granular activated carbon | 52.26 | [49] |
| Aniline | Activated carbon | 26.88 | [50] |
| Aniline | Graphene oxide | 136.98 | [51] |
| Aniline | Activated carbon | 75.75 | This study |

$K_L$ is the Langmuir constant related to the affinity of binding sites (L/mg) and computed from the plot of $C_e/q_e$ against $C_e$ which give a straight line with a slope of $1/q_{max}$ and an intercept of $1/(q_{max}K_L)$ (Fig. 9(a)).

The Freundlich isotherm is an empirical equation based on the assumption that adsorption takes place on heterogeneous surface. The Freundlich isotherm model could be written in a linear form, which was presented in Eq. (7) [45]:

$$\log q_e = \log K_f + \frac{1}{n} \log C_e \tag{7}$$

where $K_f$ and $n$ are the Freundlich constants showing the adsorption capacity (mg/g) and intensity, respectively, that were calculated from the plot of log $q_e$ vs. log $C_e$ (Fig. 9(b)).

Experimental data of aniline adsorption on both HDTMA-Bent and AC were well fitted with Langmuir model ($R^2 = 0.992$, $\chi^2 = 14$ for HDTMA-Bent and $R^2 = 0.998$, $\chi^2 = 1{,}243$ for AC) under the tested concentrations. It can be concluded that the adsorption of aniline on to both tested adsorbents is limited to the monolayer formation on a homogeneous surface. The resulting plots of and the theoretical parameters of adsorption isotherms [7,43] are presented in Fig. 9 and Table 3. Furthermore, as reported in Table 4, adsorption capacity obtained in this study is comparable with other adsorbents as reported by other researchers.

The influence of adsorption isotherm shape has been discussed [46] to examine whether adsorption is favorable in terms of "$R_L$", a dimensionless constant referred to as separation factor or equilibrium parameter. "$R_L$" is calculated using Eq. (8):

$$R_L = \frac{1}{(1 + K_L C_0)} \tag{8}$$

The value of $R_L$ indicates the adsorption nature to be either unfavorable ($R_L > 1$), linear ($R_L = 1$), favorable ($0 < R_L < 1$), or irreversible ($R_L = 0$).

The value of $R_L$ obtained for aniline was in the range of 0–1 (Table 3), suggesting that the adsorption of aniline onto HDTMA-Bent and AC is favorable. The magnitude of variation in $R_L$ ($0 < R_L < 1$) indicated that the adsorption of aniline by HDTMA-Bent and AC is thermodynamically favorable and that both adsorbents are suitable for aniline removal from aqueous solutions.

As presented in Table 3, the Freundlich constant ($K_F$) and the heterogeneity factor ($1/n$) for

HDTMA-Bent calculated from the slope and the intercept of the linear plot are 2.77 mg/g and 0.1347, and $K_f$ and $1/n$ are 11.48 mg/g and 0.340 for AC. Since the value of $1/n$ is less than 1, the adsorption of aniline onto both adsorbents is a physical process, for example, ion exchange or partition [52]. The values $1/n$ indicates favorable adsorption and that the adsorbents having a high affinity for aniline since the higher value of $1/n$ corresponded to greater heterogeneity of the adsorbent surface as previously showed in FTIR analysis. This resulted from aniline interactions with surfactant cations on the clay's surface and within the clay interlayer space for HDTMA-Bent [53].

## 4. Conclusions

The results of the study indicate that surface modification of bentonite with HDTMA enhances the aniline adsorption. The adsorption kinetic followed the pseudo-second-order model and the adsorption isotherm data fitted well to the Langmuir model with $R^2 = 0.992$ for HDTMA-Bent and $R^2 = 0.998$ for AC. Accordingly, the maximum adsorption capacity were obtained as 9.46 mg/g for HDTMA-Bent and 75.76 mg/g for AC. Although AC adsorption works well for the aniline removal and it has shown about eight times more efficiency as compared to modified bentonite in this study, but the cost of AC is high (≈US $ 4,000–4,500/ton) and bentonite is about 30–40 times cheaper than AC (≈US $ 100–150/ton), therefore, it is reasonable to conclude that bentonite can be used as a low-cost alternative adsorbent for aniline removal from water.

## Acknowledgments

The authors would like to acknowledge Hamadan University of Medical Sciences for financial and instrumental supports.

## References

[1] R. Hu, X. Wang, S. Dai, D. Shao, T. Hayat, A. Alsaedi, Application of graphitic carbon nitride for the removal of Pb(II) and aniline from aqueous solutions, Chem. Eng. J. 260 (2015) 469–477.

[2] M.A. Salam, M.A. Gabal, A.Y. Obaid, Preparation and characterization of magnetic multi-walled carbon nanotubes/ferrite nanocomposite and its application for the removal of aniline from aqueous solution, Synth. Met. 161 (2012) 2651–2658.

[3] Z. Gu, M. Gao, Z. Luo, L. Lu, Y. Ye, Y. Liu, Bis-pyridinium dibromides modified organo-bentonite for the removal of aniline from wastewater: A positive role of π–π polar interaction, Appl. Surf. Sci. 290 (2014) 107–115.

[4] S. Suresh, V.C. Srivastava, I.M. Mishra, Removal of 4-nitrophenol from binary aqueous solution with aniline by granular activated carbon using Taguchi's design of experimental methodology, Theor. Found. Chem. Eng. 47 (2013) 284–290.

[5] B. Kakavandi, A.J. Jafari, R.R. Kalantary, S. Nasseri, A. Ameri, A. Esrafily, Synthesis and properties of $Fe_3O_4$-activated carbon magnetic nanoparticles for removal of aniline from aqueous solution: Equilibrium, kinetic and thermodynamic studies, Iran. J. Environ. Health. Sci. Eng. 10 (2013) 1–9.

[6] H. Yan, X. Yang, J. Chen, C. Yin, C. Xiao, H. Chen, Synergistic removal of aniline by carbon nanotubes and the enzymes of Delftia sp. XYJ6, J. Environ. Sci. 23 (2011) 1165–1170.

[7] G.-Q. Wu, X. Zhang, H. Hui, J. Yan, Q.-S. Zhang, J.-L. Wan, Y. Dai, Adsorptive removal of aniline from aqueous solution by oxygen plasma irradiated bamboo based activated carbon, Chem. Eng. J. 185–186 (2012) 201–210.

[8] H. Al-Johani, M.A. Salam, Kinetics and thermodynamic study of aniline adsorption by multi-walled carbon nanotubes from aqueous solution, J. Colloid Interface Sci. 360 (2011) 760–767.

[9] F.J. O'Neill, K.C.A. Bromley-Challenor, R.J. Greenwood, J.S. Knapp, Bacterial growth on aniline: Implications for the biotreatment of industrial wastewater, Water Res. 34 (2000) 4397–4409.

[10] M. Leili, G. Moussavi, K. Naddafi, Degradation and mineralization of furfural in aqueous solutions using heterogeneous catalytic ozonation, Desalin. Water Treat. 51 (2013) 6789–6797.

[11] S.S.C. Karunakaran, Solar photocatalysis: Oxidation of aniline on CdS, Sol Energy 79 (2005) 505–512.

[12] J. Yao, X. Li, W. Qin, Computational design and synthesis of molecular imprinted polymers with high selectivity for removal of aniline from contaminated water, Anal. Chim. Acta 610 (2008) 282–288.

[13] M. Toor, B. Jin, Adsorption characteristics, isotherm, kinetics, and diffusion of modified natural bentonite for removing diazo dye, Chem. Eng. J. 187 (2012) 79–88.

[14] A. Bhatnagar, A. Minocha, M. Sillanpää, Adsorptive removal of cobalt from aqueous solution by utilizing lemon peel as biosorbent, Biochem. Eng. J. 48 (2010) 181–186.

[15] A. Bhatnagar, Removal of bromophenols from water using industrial wastes as low cost adsorbents, J. Hazard. Mater. 139 (2007) 93–102.

[16] F. Banat, B. Al-Bashir, S. Al-Asheh, O. Hayajneh, Adsorption of phenol by bentonite, Environ. Pollut. 107 (2000) 391–398.

[17] J. Ma, J. Qi, C. Yao, B. Cui, T. Zhang, D. Li, A novel bentonite-based adsorbent for anionic pollutant removal from water, Chem. Eng. J. 200–202 (2012) 97–103.

[18] U.F. Alkaram, A.A. Mukhlis, A.H. Al-Dujaili, The removal of phenol from aqueous solutions by adsorption using surfactant-modified bentonite and kaolinite, J. Hazard. Mater. 169 (2009) 324–332.

[19] M.V. Burmistr, K.M. Sukhyy, V.V. Shilov, P. Pissis, A. Spanoudaki, I.V. Sukha, V.I. Tomilo, Y.P. Gomza, Synthesis, structure, thermal and mechanical properties of nanocomposites based on linear polymers and layered silicates modified by polymeric quaternary ammonium salts (ionenes), Polymer 46 (2005) 12226–12232.

[20] H.B. Senturk, D. Ozdes, A. Gundogdu, C. Duran, M. Soylak, Removal of phenol from aqueous solutions by adsorption onto organomodified Tirebolu bentonite: Equilibrium, kinetic and thermodynamic study, J. Hazard. Mater. 172 (2009) 353–362.

[21] Z. Rawajfih, N. Nsour, Characteristics of phenol and chlorinated phenols sorption onto surfactant-modified bentonite, J. Colloid Interface Sci. 298 (2006) 39–49.

[22] B. Tanhaei, M.P. Chenar, N. Saghatoleslami, M. Hesampour, T. Laakso, M. Kallioinen, M. Sillanpää, M. Mänttäri, Simultaneous removal of aniline and nickel from water by micellar-enhanced ultrafiltration with different molecular weight cut-off membranes, Sep. Purif. Technol. 124 (2014) 26–35.

[23] G. McKay, M. Hadi, M.T. Samadi, A.R. Rahmani, M.S. Aminabad, F. Nazemi, Adsorption of reactive dye from aqueous solutions by compost, Desalin. Water Treat. 28 (2011) 164–173.

[24] E.M. Kalhori, K. Yetilmezsoy, N. Uygur, M. Zarrabi, R.M.A. Shmeis, Modeling of adsorption of toxic chromium on natural and surface modified lightweight expanded clay aggregate (LECA), Appl. Surf. Sci. 287 (2013) 428–442.

[25] X. Xin, W. Si, Z. Yao, R. Feng, B. Du, L. Yan, Q. Wei, Adsorption of benzoic acid from aqueous solution by three kinds of modified bentonites, J. Colloid Interface Sci. 359 (2011) 499–504.

[26] L.M. Zacaroni, Z.M. Magriotis, M. das Graças Cardoso, W.D. Santiago, J.G. Mendonça, S.S. Vieira, D.L. Nelson, Natural clay and commercial activated charcoal: Properties and application for the removal of copper from cachaça, Food Control 47 (2015) 536–544.

[27] L. Zhirong, M.A. Uddinb, S. Zhanxue, FT-IR and XRD analysis of natural Na-bentonite and Cu(II)-loaded Na-bentonite, Spectrochim. Acta Part A: Mol. Biomol. Spectrosc. 79 (2011) 1013–1016.

[28] M. Kowalska, H. Güler, D.L. Cocke, Interactions of clay minerals with organic pollutants, Sci. Total Environ. 141 (1994) 223–240.

[29] Y. Juan, Q. Ke-qiang, Preparation of activated carbon by chemical activation under vacuum, Environ. Sci. Technol. 43 (2009) 3385–3390.

[30] G.Z. Kyzas, E.A. Deliyanni, N.K. Lazaridis, Magnetic modification of microporous carbon for dye adsorption, J. Colloid Interface Sci. 430 (2014) 166–173.

[31] R. Holze, Raman spectroscopic investigation of aniline: Adsorption and polymerisation, J. Electroanal. Chem. Interfacial Electrochem. 224 (1987) 253–260.

[32] H. Koyuncu, N. Yıldız, U. Salgın, F. Köroğlu, A. Çalımlı, Adsorption of o-, m-and p-nitrophenols onto organically modified bentonites, J. Hazard. Mater. 185 (2011) 1332–1339.

[33] H. Zaghouane-Boudiaf, M. Boutahala, Adsorption of 2,4,5-trichlorophenol by organo-montmorillonites from aqueous solutions: Kinetics and equilibrium studies, Chem. Eng. J. 170 (2011) 120–126.

[34] S. Al-Asheh, F. Banat, L. Abu-Aitah, Adsorption of phenol using different types of activated bentonites, Sep. Purif. Technol. 33 (2003) 1–10.

[35] G. Zolfaghari, A. Esmaili-Sari, M. Anbia, H. Younesi, S. Amirmahmoodi, A. Ghafari-Nazari, Taguchi optimization approach for Pb(II) and Hg(II) removal from aqueous solutions using modified mesoporous carbon, J. Hazard. Mater. 192 (2011) 1046–1055.

[36] T. Anirudhan, M. Ramachandran, Removal of 2,4,6-trichlorophenol from water and petroleum refinery industry effluents by surfactant-modified bentonite, J. Water Process Eng. 1 (2014) 46–53.

[37] N. Rauf, S. Tahir, J.-H. Kang, Y.-S. Chang, Equilibrium, thermodynamics and kinetics studies for the removal of alpha and beta endosulfan by adsorption onto bentonite clay, Chem. Eng. J. 192 (2012) 369–376.

[38] Z. Aksu, Equilibrium and kinetic modelling of cadmium(II) biosorption by *C. vulgaris* in a batch system: Effect of temperature, Sep. Purif. Technol. 21 (2001) 285–294.

[39] J. Tan, X. Zhang, X. Wei, L. Wang, Removal of malachite green from aqueous solution using waste newspapaer fiber, Bioresources 7(3) (2012) 4307–4320.

[40] H. Zhu, R. Jiang, L. Xiao, W. Li, A novel magnetically separable $\gamma$-$Fe_2O_3$/crosslinked chitosan adsorbent: Preparation, characterization and adsorption application for removal of hazardous azo dye, J. Hazard. Mater. 179 (2010) 251–257.

[41] S. Lagergren, About the theory of so-called adsorption of soluble substances, K. Svenska Vetenskapsakad Handl 24 (1898) 1–39.

[42] Y.-S. Ho, G. McKay, Pseudo-second order model for sorption processes, Process Biochem. 34 (1999) 451–465.

[43] B. Tang, Y. Lin, P. Yu, Y. Luo, Study of aniline/ε-caprolactam mixture adsorption from aqueous solution onto granular activated carbon: Kinetics and equilibrium, Chem. Eng. J. 187 (2012) 69–78.

[44] F.W. Pontius (Ed.), Water Quality and Treatment, McGraw-Hill Inc., New York, NY, 1990, pp. 781–876.

[45] H.M.F.Freundlich, Over the adsorption in solution. J. Phys. Chem. 57 (1906) 385–471.

[46] T.W. Weber, R.K. Chakravorti, Pore and solid diffusion models for fixed-bed adsorbers, AIChE J. 20 (1974) 228–238.

[47] Y. Xi, M. Mallavarapu, R. Naidu, Preparation, characterization of surfactants modified clay minerals and nitrate adsorption, Appl. Clay Sci. 48 (2010) 92–96.

[48] J. Su, H.-G. Huang, X.-Y. Jin, X.-Q. Lu, Z.-L. Chen, Synthesis, characterization and kinetic of a surfactant-modified bentonite used to remove As(III) and As(V) from aqueous solution, J. Hazard. Mater. 185 (2011) 63–70.

[49] A.J. Jadhav, V.C. Srivastava, Adsorbed solution theory based modeling of binary adsorption of nitrobenzene, aniline and phenol onto granulated activated carbon, Chem. Eng. J. 229 (2013) 450–459.

[50] D.M. Nevskaia, E. Castillejos-Lopez, A. Guerrero-Ruiz, V. Muñoz, Effects of the surface chemistry of carbon materials on the adsorption of phenol–aniline mixtures from water, Carbon 42 (2004) 653–665.

[51] A. Fakhri, Adsorption characteristics of graphene oxide as a solid adsorbent for aniline removal from aqueous solutions: Kinetics, thermodynamics and mechanism studies, J. Saudi Chem. Soc. (in press), doi: 10.1016/j.jscs.2013.10.002.

[52] J.-Q. Jiang, C. Cooper, S. Ouki, Comparison of modified montmorillonite adsorbents: part I: Preparation, characterization and phenol adsorption, Chemosphere 47 (2002) 711–716.

[53] L. Zhu, R. Zhu, Simultaneous sorption of organic compounds and phosphate to inorganic–organic bentonites from water, Sep. Purif. Technol. 54 (2007) 71–76.